ICEMS

2010 International Conference on Electrical Machines and Systems

October 10-13, 2010, Songdo Convensia, Incheon, Korea

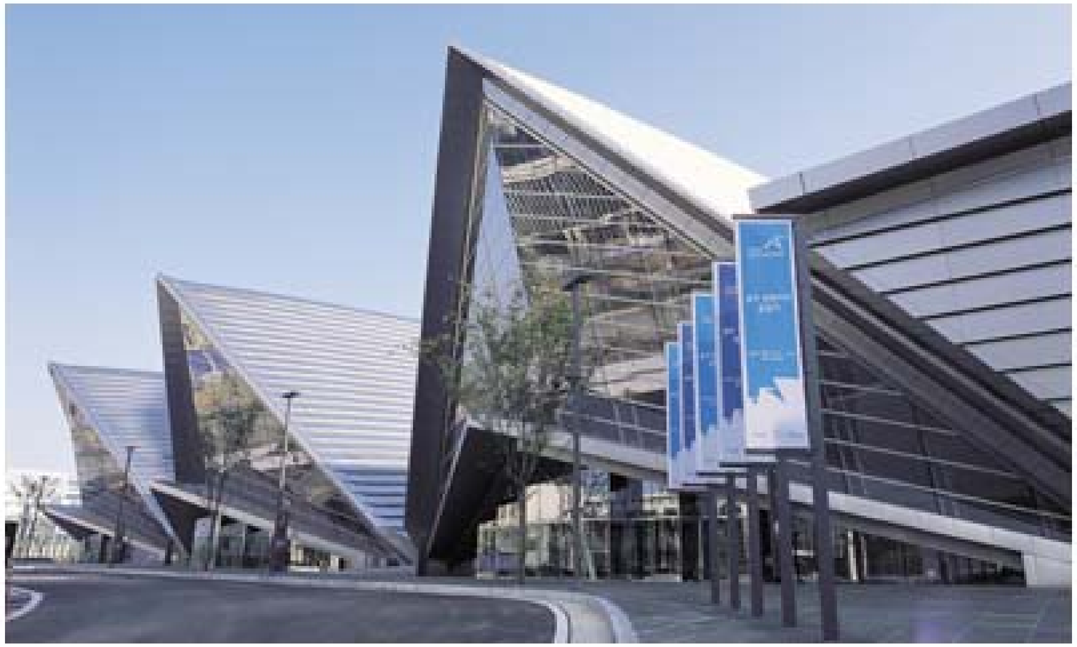

IEEE Catalog Number: CFP10801-CDR
ISBN: 978-89-86510-12-6
Vendor: Prof. Jin Hur
Tel: +82-52-259-1282 / Fax: +82-52-259-1686
E-mail: jinhur@ulsan.ac.kr

Organized by

KIEE (The Korean Institute of Electrical Engineers)

Co-organized by

CES (China Electrotechnical Society)
IEEJ (The Institute of Electrical Engineers of Japan)

Technical Co-sponsor

IEEE IEEE Industry Application Society

Jung-Pyo Hong

- The Effect of Silicon Steel Sheet on Core Loss in Induction Motor

Jung-Pyo Hong

- Effect of Vibration and Noise on IPMSM Type Integrated Starter and Generator According to Number of Slots

Jung-Pyo Hong

- Reduction Design of Eddy Current Loss in IPMSM using Response Surface Methodology

Jung-Pyo Hong

- A Study on the Relation Between Rotor Rib and Maximum Power of IPMSM in Flux Weakening Region

Jung-Pyo Hong

- Design of an Interior Permanent Magnet Synchronous In-Wheel for Electric Vehicles

Jung-Pyo Hong

- Vibration Analysis according to Stator Shape Design in a PMSM

Jung-Pyo Hong

- Characteristic Analysis of the Water Pump Motor considering Polar Anisotropic Ferrite Bonded Magnet

Jung-Pyo Hong

- A Study on the Reduction of Noise and Vibration of SPM According to Reduction of Permanent Magnet

Jung-Pyo Hong

- Evaluation and Improved Design about Acoustic Noise and Vibration in IPMSM

Jung-Pyo Hong

- Reduction Eddy Current Loss Design and Analysis of In-Wheel Type Vehicle Traction Motor

Characteristic Analysis of the Water Pump Motor considering Polar Anisotropic Ferrite Bonded Magnet

Su-Jin Lee[1], Sung-Il Kim[1], Jung-Pyo Hong[1], Byoung-Young Song[2], Jong Won Park[2]
[1]Dept. of Automotive Engineering, Hanyang University, Seoul, Korea
[2] R&D Team, GMB Korea Corp., Changwon, Korea
E-mail: issue@hanyang,ac,kr, hongjp@hanyang.ac.kr

Abstract — This paper deals with the characteristic analysis of the water pump motor considering polar anisotropic ferrite bonded magnet in an outer-rotor type Brushless DC motor(BLDC). The characteristic analysis of BLDC motor utilizing the plastic magnet without rotor core has been performed by using finite element analysis (FEA). Besides, in the analysis, the overhang effect of the magnet is calculated by using 3D FEA. The validity of the analysis method is verified by comparing the analyzed results with measured ones.

I. Introduction

Around the world, as the interest about the air pollution is increasingly raised, the engine and automobile parts can be satisfied with the environmental regulations have been demanded. Traditional automotive water pumps are belt driven by the vehicle engine, constraining pump shaft speed operate at engine speed multiplied by the belt speed ratio. Because such a mechanical water pumps have a structure that the speed control of mechanical water pump is difficult. Traditional water pump are run continuously during engine operation and utilize a thermostat-controlled by pass when engine cooling is not required. Therefore a decrease output power and an increase of fuel are occurred due to the consumption of needless power.

Then in order to solve these problems, electric water pump is introduced. The electric water pump can provide constant input speed, and also consumes less energy by only pumping when needed. Using electric water pump system can reduce the operating loss, which is benefit for the environment [1]. Consequently, development of technology about electric water pump is needed for Idle Stop and Go (ISG) and hybrid car.

Recently, Brushless DC motor (BLDC) have long life and haven't the additional cost for maintenance are widely used for many applications in the automobile [2]-[4]. In order to increase surface magnetic fluxes and to obtain rectangular flux density waveform, plastic magnets are magnetized with polar shape. Besides, BLDC motors with polar plastic magnets can not have a rotor core in order to reduce manufacturing cost and inertia of the rotating part.

In this paper, the characteristic analysis of an outer-rotor type, BLDC motor considering polar anisotropic ferrite bonded magnet are analyzed by using finite element method (FEM). Length of the rotor stack in this motor is longer than stator, its have the overhang effect of magnet. So, due to accretive analysis results, the overhang effects are calculated by using 3-D FEM. Furthermore, owing to the verification of analysis, the proposed method is substantiated by comparing the analyzed results with the measured one.

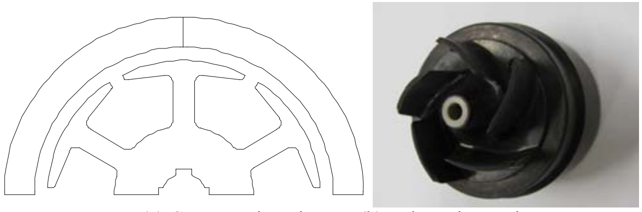

(a) Cross-section view (b) Polar anisotropic magnet

Fig.1. The configuration of the analyzed motor.

TABLE I
SPECIFICATION OF THE ANALYSIS MODEL

Section	Item (Unit)	Value
Stator	Number of phases	3
	Number of slots	6
	Stack length (mm)	15
	Number of turn per phase (turn)	118
Rotor	Number of poles	4
	Stack length (mm)	17
	Br (T)	0.267
PM	Residual induction (T)	0.267
	Coercive force (kA/m)	183
	Maximum energy product (kJ/m^3)	14.0
	Need magnetizing field intensity(kA/m)	over than 550
Air gap	Mechanical air gap (mm)	1.8

II. Structures and Magnetization Modeling

A. Specification of the analysis model

Fig.1 shows the cross-section view of the outer-rotor type BLDC motor. Its rotor hasn't the rotor yoke and is magnet including the impala. This motor is driven by 120° square wave current source and sensor less drive. Table 1 shows the specifications of the analysis model.

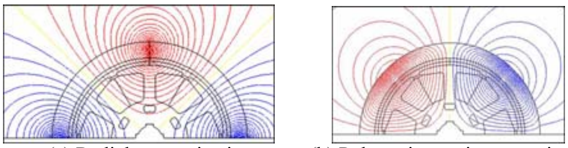

(a) Radial magnetization (b) Polar anisotropic magnetization

Fig.2. Equi-potential and flux distribution of magnet according to magnetization distribution.

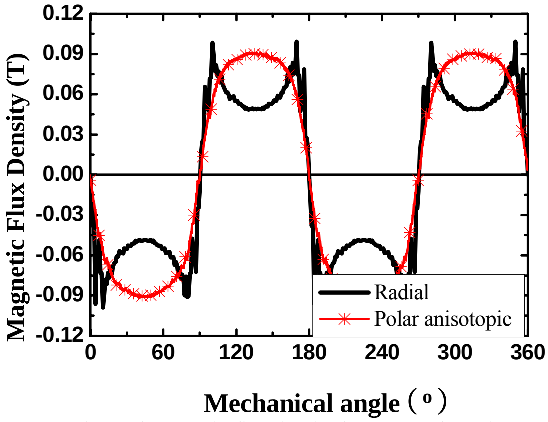

Fig. 3. Comparison of magnetic flux density between polar anisotropic and radial magnets

B. Analysis Method

For the analysis, 2D-FEM is used. A magneto-static analysis is used to determine the magnetization of magnet, and a voltage source transient analysis using time-stepping FEM is used to analyze the performances of the BLDC motor. The governing equation for analyzing the magnetic field distribution of the structure of the mold for this polar anisotropic plastic magnet is given by (1) [5]. Since the magnetic field inside the structure of the injection mold is produced by permanent magnet, there is no forced current and no eddy current, and the analysis becomes a two dimensional static magnetic field analysis.

$$\frac{\partial}{\partial x}\left(\frac{1}{\mu}\frac{\partial A_z}{\partial x}\right)+\frac{\partial}{\partial x}\left(\frac{1}{\mu}\frac{\partial A_z}{\partial y}\right)=-J_o-\frac{1}{\mu}\left(\frac{\partial M_y}{\partial x}-\frac{\partial M_x}{\partial y}\right) \quad (1)$$

where A_z is the z-component of magnetic vector potential, J_o is the input current density and M_x, M_y are the x- and y-component of magnetization of permanent magnets.

From the analysis of the magnetization model, the flux density vectors $B^{(e)}$ of each element in bonded magnet region are obtained. The magnetization directions of the anisotropic ferrite material are arranged to same directions as external flux. So, the magnetization directions, $\theta^{(e)}$, of the magnet are determined by (2) in each element.

$$\theta^{(e)}=\tan^{-1}\frac{B_y^{(e)}}{B_x^{(e)}} \quad (2)$$

In the FEM considering the magnetization distributions, the values and directions of magnetization of each element are determined by (3) and (4).

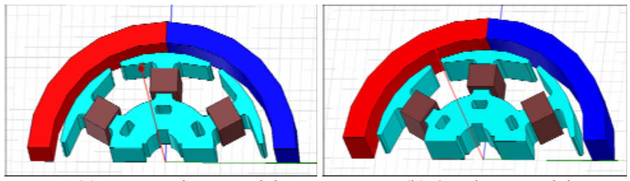

(a) Non overhang model (b) Overhang model

Fig. 4. Analysis model for calculation of overhang effect using the 3-D FEM

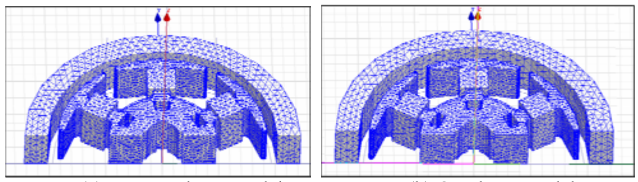

(a) Non overhang model (b) Overhang model

Fig. 5. Finite element meshes of the analysis 3-D model

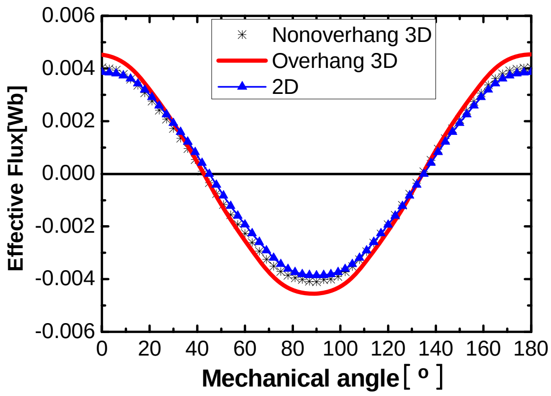

Fig. 6. Comparison of the flux linkage at the winding according to the overhang

$$M_x^{(e)}=M_r^{(e)}\cos\theta^{(e)} \quad (3)$$

$$M_y^{(e)}=M_r^{(e)}\sin\theta^{(e)} \quad (4)$$

where M_r is the residual magnetization of the ferrite magnet material indicated in the specification, and M_x, M_y are the x- and y- component of magnetization of each element. In the two-dimensional FEM analysis, the magnitude $M_r^{(e)}$ of the magnetization $M^{(e)}$ for every element of the plastic magnet portioned in one-dimensional triangular elements is determined by the magnitude $B_r^{(e)}$ of the magnetic flux density $B^{(e)}$ of that element.

III. Analysis Results and Discussion

Fig.2 shows the flux distributions of the magnet according to magnetization distributions, that is, one is the case of radial magnetization with constant intensity and the other is the case that have analyzed magnetization distributions. We can see that the flux patterns are very different.

Fig.3 compares magnetic flux density, radial magnets with polar anisotropic magnets. It can be seen that surface magnetic flux density from the polar anisotropic magnet is 25% higher than that of radial magnet. The performances of the BLDC motor employing the fabricated polar anisotropic magnet are also improved compared with motor employing radial direction magnets. So, we study the characteristic analysis of

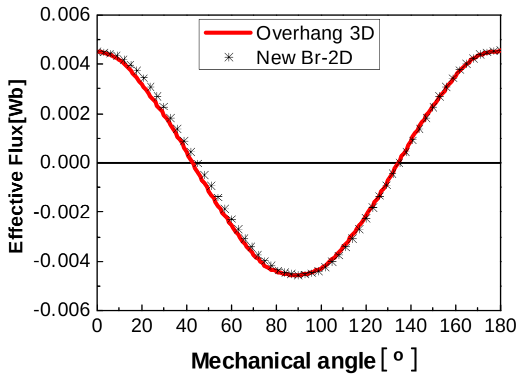

Fig. 7. Comparison of the flux linkage at the winding according to between the overhang model(3D-FEM) and new Br 2D-FEM

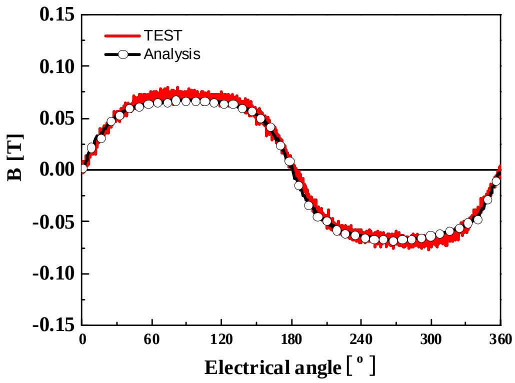

Fig. 8. Surface flux density distribution of bonded magnets in air

the water pump motor considering polar anisotropic ferrite bonded magnet for higher power.

In this model, the axial length of the magnet is longer than that of stator core in order to increase the effective magnetic flux. So, in 2-D FEM, the overhang effect must be considered. In this paper, the overhang effect is calculated by using 3-D FEM. Fig. 4 shows the 3-D analysis model, one has not magnet overhang and the other has real magnet overhang. Fig. 5 show finite element meshes of the analysis 3-D model. From the comparison of the flux linkage at the winding region, the overhang effect can be calculated. Fig. 6 shows the comparison of the flux linkage at the winding according to the overhang. For the calculation of the overhang effect, we used a commercial 3-D FEM software “Maxwell 3D”. The increase rate of flux linkage flux to the magnet overhang is 1.723. So, in 2-D FEM of the BLDC motor, we increased the residual flux density to 1.723 times. The analysis result considering the overhang effect is shown the Fig. 7. Fig. 7 show comparison of the flux linkage at the winding according to between the overhang model and new – Br 2D FEM.

The magnetic properties of the ferrite bonded magnets were measured by using a flux meter after magnetization. Fig. 8 compares the measured values and the analytical values of the radial components of the surface flux densities of the magnet. Both agree very well and show that the orientation of the polar anisotropic plastic magnet determined by this analysis is appropriate. Consequently, the validity of the analysis method is verified by comparing the analyzed results with measured ones.

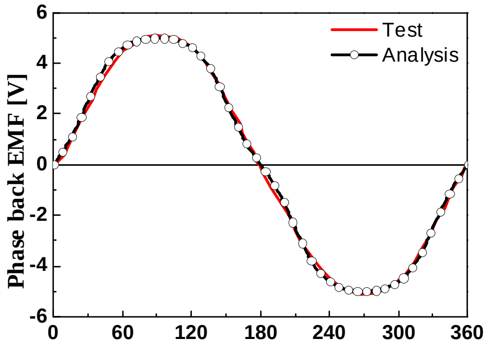

Fig. 9. Phase back EMF waveforms in case of 4300 rpm

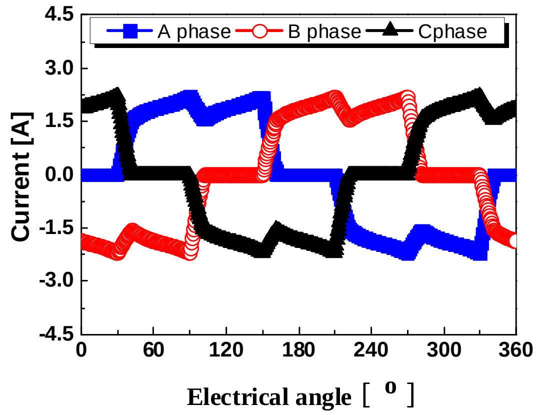

Fig. 10. Input current wave form

Fig. 9 shows the analysis and measured results for phase back EMF wave forms of the BLDC motor at the speed of 4300rpm. We can see that profiles and values of the analyzed and measured results are very close. In case of polar magnetization, because of the sinusoidal air-gap flux density distributions of the bonded magnet, the EMF waveform is close to the sine wave. Fig. 10 shows the input current wave at rated number of rotations 2700rpm and Fig. 11 show the torque waveforms ate the respective number of rotations analyzed with dc source voltage of 12. The average torque at rated point is 0.032 Nm in case of polar anisotropic plastic magnets.

Fig. 12 shows the determined results of the torque-speed characteristics with the average value of the instantaneous torques at the number of rotations. No-load speed is 5000rpm, stall torque is 0.088Nm. Table 2 shows the analysis results of the BLDC motor.

IV. Conclusion

In this paper, we analyzed an outer rotor type BLDC motor that does not have a rotor core. This paper deals with the characteristic analysis of the water pump motor considering polar anisotropic ferrite bonded magnet in an outer-rotor type BLDC motor. By performing the magnetic field analysis by FEM, the orientations which are different for all parts are determined accurately. The validity of the analysis method is verified by comparing the analyzed results with measured ones. We confirm that out analysis method is useful for analysis and design of many electromagnetic machines.

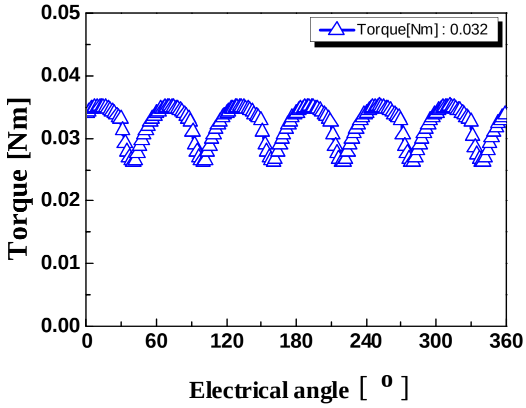

Fig. 11. The result of the torque analysis using the FEM

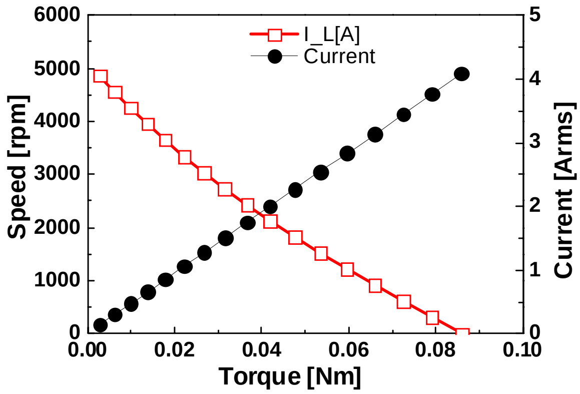

Fig. 12. T-N-I curve data of the analysis BLDC motor

TABLE II
ANALYSIS RESULT OF THE BLDC MOTOR

	Value	Note
DC Link Voltage [V_{DC}]	12	- Modulation 0.96
Lead angle [˚]	0	
Coil Diameter [mm]	0.5	
Resistance [Ω]	1.194	
Self Inductance [mH]	611.2	
Mutual Inductance [mH]	277.2	
Input Current [A_{rms}]	1.52	
Current Density [A/mm^2]	7.74	
Torque [Nm]	0.032	
Torque ripple [%]	27.76	
Speed [rpm]	2700	
Output Power [W]	9.05	

REFERENCES

[1] Harris N. C., Jahns T. M., Suroug Huang "Design of an integrated motor/controller drive for an automotive water pump application," *in conf. Rec. IEEE-IAS Annu Meeting*, vol.3, pp.2028-2035, 2002

[2] J. Ormerod and S. Constantinides. "Bonded permanent magnets: Current status and future opportunities," *J. Appl. Phys.*, vol.8, no.8, pp.4816-4820, 1997.

[3] W. –B. Tsai and T.-Y. Chang, "Analysis of flux leakage in a bushless permanent magnet motor with embedded magnets." *IEEE Trans on Magn.*, vol. 35, no. 1, pp.543-547, 1999

[4] M. Jeon, D. Kim, C. Kim, "Optimum Design of BLDC Motor for Cogging Torque Minimization Using Genetic Algorithm and Response Surface Method," *Journal of Electrical Engineering&Technology*, vol. 1, no. 4, pp. 466-471, 2006.

[5] Kitamura, Ishihara, Todaka, Inoue, "Magnetic field analysis of dc brushless motor considered volt-ampere characteristic of feedback diodes," *Trans. IEE Jpn*, pp. 1268-1275, 1996

[6] S. B. Yoon, I. S, Jung, K. C. Kim, and D. S. Hyun, "Dynamic analysis of a reciprocating linear actuator for gas compression using finite element method," *IEEE Trams. On Magn.*, vol. 33, no. 5, pp. 4113-4115, 1997